International Journal of Multicultural and Multireligious Understanding

http://ijmmu.com
editor@ijmmu.com
ISSN 2364-5369
Volume 7, Issue 11
December, 2020
Pages: 503-516

Investigation of the Use of Titanium Dioxide Nanoparticles in Solar Cells

Chen Luo[1]; Jingting Li[1]; Jie Xu[2]

[1] Shenzhen Key Laboratory of Advanced Thin Films and Applications, College of Physics and Optoelectronic Engineering, Shenzhen University, 518060, People's Republic of China

[2] China Academy of Engineering Physics (CAEP), PO. Box 919-988-5, Mianyang 621900, People's Republic of China

http://dx.doi.org/10.18415/ijmmu.v7i11.2166

Abstract

Today, nanoparticles have attracted the attention of many researchers due to their special properties as well as their many technological applications. Among these, titanium dioxide nanoparticles have many important applications in various industries due to their excellent optical, electrical and catalytic properties. These applications include use in industrial pigments, as photocatalysts in environmental cleansing, in sunscreens to protect the skin, in photovoltaic applications for solar cells, sensors, in electronic device components, and many more. Two important properties of this material that make it very efficient and useful in life are its photocatalytic and superhydrophobic properties. These two properties are used to purify water and wastewater, eliminate air pollution and buildings, accelerate photochemical reactions such as hydrogen production, fabricate surfaces and layers and self-cleaning glass. The properties of titanium dioxide nanoparticles are strongly dependent on the size of the doped particles, elements or compounds and the surface modifications made on them, which in turn are influenced by the nanoparticle synthesis method. For this reason, methods for the synthesis of titanium dioxide nanoparticles have received much attention today. As the size of the material gets smaller and smaller and reaches the nanoscale, new physical and chemical properties show up. Among the unique properties of nanomaterials, the motion of electrons and holes in semiconductor nanomaterials is dominated by quantum constraint, and the transfer properties of phonons and photons are strongly influenced by the size and geometry of the material. The effective surface area and surface to volume ratio increase with decreasing the material size. High effective levels are achieved by small particles, which will be useful in many 2TiO-based types of equipment in which the interaction of the common surface of the material is important.

Keywords: *Solar Energy; Titanium Dioxide Nanoparticles**;** Solar Cells; Titanium Dioxide*

Introduction

Knowing the energy of the sun and using it for various purposes dates back to prehistoric times. Perhaps the pottery era, when the temple clerics were cycled with large golden cups and used the sun's

rays to light the altars' fireplaces. Or in the time of the Egyptian pharaohs in the period of Amenhotep III (1419-1455 BC) due to sunlight on the talking statues, the air inside them was hot. The statues were sounded. Also, above the tomb of Mamnan, son of Amenophis, a bird was installed, which was sounded by the morning sun [1]. The most important account of the use of solar radiation is the story of Archimedes, the great scientist and inventor of ancient Greece (212-287 BC) [2]. They set fire to the Roman fleet using the sun's thermal energy. Archimedes is said to have focused the sun's rays on Roman ships from a distance by setting a large number of small square mirrors next to each other on a movable pedestal, setting them on fire. For this reason, Archimedes is mentioned as the founder of the use of solar radiation. At the same time, Egyptian sources are older than that. The Romans write in history that they were defeated by an invisible force and believed that they were at war with the gods. The question is whether Archimedes knew enough about optics or used a simple method to concentrate the sun's rays at one point. It seems that this scientist had written a book called incendiary mirrors. However, unfortunately, there is no copy of it to clarify the matter. The book may have been destroyed in a Roman invasion a few years later that led to the conquest of Greece, as the Romans killed Archimedes himself [3]. About 1800 years after Archimedes, a person named KITCHER (A.KIRCHER, 1610-1680) repeated Archimedes' masterpiece and, using several mirrors, set fire to a wooden anchorage from a distance and proved that the story was true. In 1615, SALMON DE CAUM, a Frenchman, proclaimed the solar engine. Using several lenses mounted in a frame, he focused the sun's rays on a closed metal cylinder, part of which was filled with water. Sunlight warmed the air inside the cylinder, and as the air expanded, the pressure inside the chamber increased and water was expelled. Although this device had a toy aspect, it was not ineffective in creating interest in using solar energy. In the 18th century, Natura built the first solar oven in France [4]. His largest furnace consisted of 360 small flat mirrors, each focusing the sun's rays independently on a single point. The researcher also designed and built a smaller furnace consisting of 168 pieces of mirrors in 1747, with which he set fire to a wooden mound 60 meters away. Solar cookers were first made by a man named (SAUCCER NICHELAS DE 1740-1799). His stove consisted of an insulated box with a black plate made up of pieces of glass with a lid on it. The sun's rays entered the box through the glass and were absorbed by the black surface and increased the temperature inside the box to 88 ° C. Anthony Lavoisier (1794-1794), the creator of modern chemistry, researched solar furnaces to obtain the most energy from the purest heat source. And built a furnace that used two plates of glass filled with alcohol between the two plates to form a convex lens. The liquid lens was 130 cm in diameter and 320 cm focal length. Because the refractive power of this liquid lens was not effective in obtaining high temperatures at its focal point, Lavazie placed another small lens at its centre. By reducing the effective focal length, the device was able to melt even platinum at 1760 ° C. BESSMER (1813-1898), the father of world steel, supplied the heat needed for his furnace using solar energy. In the nineteenth century, attempts were made to convert solar energy into other forms of energy, such as steam generation and use in steam engines [5]. During these years, several solar steam engines were built and tested. In 1878, MOUCHOT designed the first solar collector with a conical focus. The mirrors inside the cone focused all the sun's rays at a point in the middle of the incomplete cone where an absorber was installed. This collector was called AXICON. The first large axicon to be made consisting of a silver plate with a diameter of 540 cm and a surface of 18.2 m2. It weighed about 1400 kg with all the moving parts and was able to absorb 78% of the radiated solar energy [6]. But because in this design the sun's radiation was concentrated on one surface instead of one point, it was less intense. The power output of the incomplete much cone was enough to start a 1.5 kW heater, which delivered almost only 3% of the absorbed energy. At the same time, coal steam machines were able to deliver 9% to 11% of the energy received. Over the years, energy from the sun has been used in cases such as printing presses or distilling and desalinating water. Erickson, the inventor of the hot air engine cycle, received the power he needed for his experiments with a parabolic concentrator, which received about 0.7 kw of energy with a reflectance of 9.3 m3. In 1880, the first solar bed collector was built by Charles TELIER. In 1888, E-WESTER proposed the use of solar energy in thermocouples. Thus, by concentrating solar energy on thermocouples and using the basis of their work and by creating hot and cold sources, it created electrical energy at both ends of nickel and iron wires. In the nineteenth century, solar desalination devices became

popular, and devices were developed that could produce about 20,000 litres of distilled water per day on a sunny day. In the twentieth century, the use of collectors to generate steam in power plants has been considered [2]. Heating buildings using solar energy was a new idea that emerged in the 1930s and made significant progress in a decade. The first solar house was built in 1938 at the Massachusetts Institute of Technology (MIT). Advances in the design and construction of solar homes and water heaters were so rapid that it was thought that by 1970, millions of homes in various countries would be heated by solar energy. But statistics show that solar heating was even lower in the 1970s than in 1955. The high initial cost of such systems, as well as the cheap supply of oil and gas [7-9], had hindered the development of these systems. One of the most demerits of fossil fuels is the storage problems like shell damage during corrosion or buckling, which lead to many environmental problems [10-15]. There are many renewable and new generation energy sources like solar energy, and solid-state electrocatalysis plays a crucial role in the development of renewable energy to reshape current and future energy needs [16-17]. But the energy crisis of 1974 and the advancement of various solar collector construction techniques, and the possibility of reducing or depleting some underground resources, have once again drawn the world's attention to solar energy. And many efforts are made in most of the different countries of the world to develop and advance this technique. Nowadays, solar energy is used by different systems for different purposes, the most important of which are [18]:

Photobiological systems: Changes in the life of plants and organisms caused by sunlight and photosynthesis, the process of decomposing animal manure and using its gas.

Photochemical systems: Chemical changes due to sunlight- Optical electrolysis- Electrochemical photovoltaic cells- Hydrogen production facilities.

Heating and refrigeration systems Includes spa supply systems- Heating and cooling of buildings- Freshwater supply of transmission and pumping systems- Green space production systems (greenhouses)- Dryers and solar cookers- Cooling systems- Power towers- Solar dryers- Solar power plants.

Photovoltaic systems: Conversion of solar energy into electrical energy- Solar cells.

Energy consumption in buildings is on the rise due to a variety of factors such as climate change, increase in household energy consumption, growth in real estate sector, diversity of modern home appliances, variations in industry structure, excessive energy consumption in current buildings, as well as inadequate government oversight [19]. Building thermal control, in many aspects, it could be used as an energy source for heating or cooling, underfloor air distribution [20], lighting, and so forth. There are much research has been conducted on many aspects. Wide range of applications and growing usage of these type technologies is rooted in the merits of nanostructures. Vast majority of research is in this field about; Nanocrystalline [21-22], nanocomposite [23-24], Nanoparticles [25], Nanostructure [26], nanoemulsifiers [27-28]. Different materials with different particles have a wide range of properties. Therefore, the catalytic analysis is of high significance to be evaluated [29]. Therefore, synthesis of TiO_2 nanomaterials, including nanoparticles, nanorods, nanowires, nanotubes is classified according to the method of their preparation.

2. *Titanium Dioxide*

2.1. *Crystal Structure*

Titanium dioxide has three crystalline forms, including anatase, rutile and brookite [30]. Thermodynamically, rutile is the most stable phase of titanium dioxide at normal pressure, and the other two phases are the semi-stable phases of this system. The crystal base units in all three phases are 6TiO octagons. The difference between these three phases is in the arrangement of these octagons (Figure 1).

These structures are related to mass 2TiO. Due to the very high surface-to-volume ratio of 2TiO nanoparticles, the surface arrangement may vary from mass to mass.

2.2. *Fuzzy Transformation of Anatase to Rutile*

It usually crystallizes in the form of anatase phase at low temperatures. As the temperature rises, the semi-stable phase of anatase in a transformation changes to the stable phase of rutile. For bulk 2TiO, this transformation usually occurs at temperatures above 800 ° C. When the particle size decreases to the nanometer range, the transformation temperature begins to decline relative to the mass state, and the transformation temperature range expands [31].

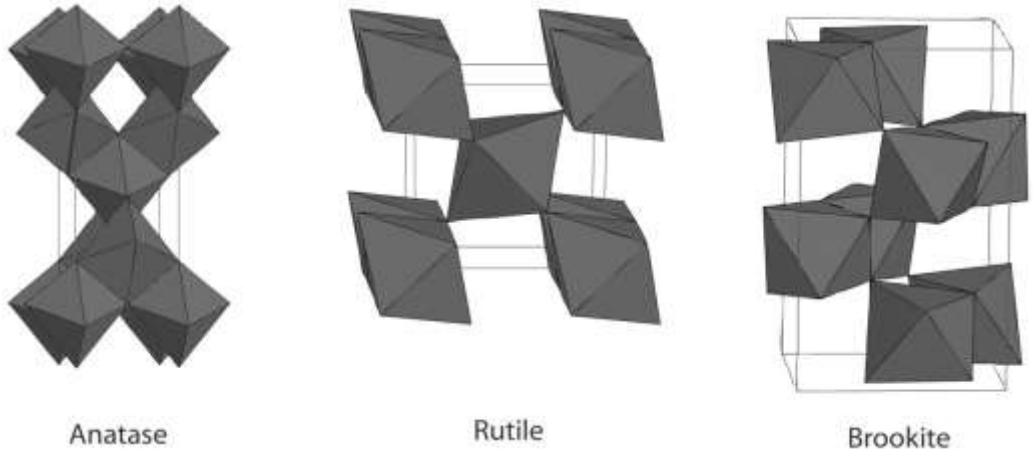

Fig 1. The arrangement of 6TiO octagons in three phases of Rutile, Anatase and Brockite [30]

3. Methods for the Synthesis of Nanostructured Titanium Dioxide

3.1. Sol-Gel Method

The sol-gel method is an easy process for making various ceramic materials. In the sol-gel method, a colloidal suspension or sol is formed from the hydrolysis and polymerization reactions (condensation) of precursors such as inorganic metal salts or organic metal compounds such as metal alkoxides [32]. Complete compaction and loss of solvent cause the transition from liquid to solid cell phase. These thin films can be obtained on a substrate by rotational coating or immersion. Considering that different coatings have specific characteristics [33]. When the cell (casting) is compressed, a wet gel will form, and this wet gel will turn into a dense ceramic by drying and heating. A material with high porosity and very low density is called argol.

3.2. Hydrothermal Method

The hydrothermal method is used only for the synthesis of simple oxide powders and mixed with controlled morphology, at a relatively low temperature (100-150 ° C). In hydrothermal processes, oxidized nanoparticles are generally synthesized by heating them in an autoclave after preparing a cell from a solution. Given that many parameters are involved in the hydrothermal process (temperature, pressure, the concentration of reactants and pH of the solution) and also that this process consists of a

heating step, Therefore, researchers have used different combinational models of these parameters in other hydrothermal methods for the synthesis of TiO_2 nanoparticles [34]. The hydrothermal method allows the synthesis of TiO_2 nanoparticles with a minimum size of 8 nm and various shapes.

3.3. Mechanochemical Method

In this method, mechanical energy activates the chemical reaction. This reaction involves the chemical reduction of metal compounds by a reducing agent during milling. Plush and Blake used the mechanochemical method to synthesize TiO_2 nanoparticles from 4TiCl liquid and 3CO (NH4) 2CO powder using an alumina chamber and pellets for milling [35]. After annealing these particles at different temperatures (230-750 ° C), nanocrystalline particles were obtained almost spherical with an average size of 10-50 nm.

3.4. Radiofrequency Thermal Plasma Method

In this method, the precursor used is evaporated by radiofrequency thermal plasma and nanoparticles are prepared from the vapour phase by performing a chemical reaction [5]. This type of plasma can be used to synthesize nanoparticles of many minerals (such as titanium nitride) and organic matter (such as titanium butoxide). The extremely high cooling rate and high concentration of reactive radicals in the plasma medium make this method a unique process for the synthesis of nanoparticles.

3.5. Chemical Vapour Condensation Method (CVC)

In this method, nanoparticles are synthesized by chemical precipitation from the vapour phase, at low pressure or atmospheric pressure. This method is very suitable for the synthesis of very fine non-agglomerated nanoparticles with high purity and excellent application properties. This process also has the potential for industrialization compared to other methods of heater synthesis [32].

3.6. Micro Mixing Method

In this method, one phase on a micron-scale is dispersed into another phase, and the amount of mixing can be controlled by the flow rate, the size of the surface-activating membrane holes and the viscosity. This method is called micromixing and has the potential to control grain-size by controlling the amount of mixing. Chen et al. Injected two solutions of titanium sulfate ($Ti(SO_4)_2$) and a solution of ammonium bicarbonate NH_4NO_3 with different concentrations into the device by two pumps. After micron penetration of one of the solutions from inside the microstructure into the other solution, a gel was synthesized, which was separated from the centre by an evaporator and dried after several washes. It was then annealed in an oven to obtain TiO_2 nanoparticles.

3.7. Solothermal Method

The solothermal method is similar to the hydrothermal method, except that the solvent used here is non-aqueous. Besides, the temperature can be higher than the hydrothermal method, and a solvent with a high boiling point can be selected. With this method, the size and shape of nanoparticles can be better controlled. The materials to be used as surface or surfactant must have specific properties [35]. The solothermal method is smaller for the synthesis of nanoparticles and nanorods and nanowires of titanium

dioxide with (and without) surfactant. Also, the crystal phase, diameter and length of the nanorods are strongly influenced by the weight ratio of the precursor/surfactant / solvent.

3.8. Neural Networks

Neural network that is a numerical modeling technique is used for estimating daily GSR. NNs can accommodate multiple input variables to predict multiple output variables. They differ from statistical modeling approaches in their ability to learn about the system that can be modeled without prior knowledge of the process relationships. The selection of anappropriate neural network topology is important in terms of model accuracy and modelsimplicity. In addition, it is possible to add or remove input and output variables in the NN algorithm if it is needed [37-38].

3.9. Method of Physical Accumulation of PVD Steam

In this method, the materials are first evaporated and then compacted in solid form. The physical vapour deposition (PVD) process was initially used only to vaporize metals by vacuum transfer without chemical reaction [39]. The PVD system and process are very efficient. They cover a wide range of variables, some of which include chemical reactions. This process is used to produce deposits of pure metals, alloys, compounds and ceramics on almost different types of substrates with different shapes [40]. The speed of coating formation in this method reaches up to 50 microns per minute. The scope of application of this method in all fields of industry and technology to create surface properties such as electrical, optical, mechanical, chemical and. The most important physical methods in making thin layers are:

- Thermal evaporation method
- Dispersion method (sputtering)

The heat evaporation method uses a steam source and a substrate in a vacuum chamber. The chamber is usually drained to a pressure of less than 5 to 10 nodes. The steam source is usually a heated plant. In this way, the coating material becomes vapour, and the vapour atoms move in a straight line to the substrate, condense on it and precipitate. Thermal evaporation of materials is done in different ways, including:

- Resistance heat source
- Instant evaporation method
- Evaporation using an electric arc
- Wire blasting method
- Laser evaporation
- Use of electronic bombardment

Dispersion method: In this method, a sample of the coating material and substrate is placed in a vacuum chamber. The chamber is emptied to a pressure of 5 to 10 torque or less. Then a neutral gas, usual argon, is sent into it so that the pressure increases to 2 to 10 torque or more. The ground sample (target) that is insulated from the ground is connected to an electrical source with a negative 3000 volts. Applying this voltage causes the severe electrical discharge. The result is an aura of argon ions. The argon ions produced are absorbed on the coating sample or targeted with high energy, and the coating sample atoms are separated by a torque transfer process. The released particles move to the bottom of the layer and condense on it to form a coating. The distribution method is done in two main ways:

- Non-reactive
- Reaction

The non-reactive process is similar to the above descriptions, but the reaction processes themselves are performed in the following ways:

- Diode distribution
- RF distribution
- Triod scattering
- Magnetron scattering
- Unbalanced magnetron scattering

4. *Properties of TiO2 Nanomaterials*

4.1. *Structural Properties of TiO2 Nanomaterials*

The structure of anatase and rutile can be considered as an octahedral chain in which each $^{4+}$Ti ion is surrounded by 6 $^{2-}$O ions. These two crystals are different in terms of torsion (angular strain) of the chains. In the rutile structure, the octagon shows a right-angled twist. In contrast, in the anatase structure, the octagon is significantly twisted, so its symmetry is less than that of the right angle. The Ti-Ti distance in anatase is larger while the Ti-O length is shorter than in rutile. In the rutile structure, each central atom is associated with ten close neighbours, while in anatase there are eight close neighbours. These differences in the structure of the network cause differences in the mass density and electronic band structures of these two forms of 2TiO. So that the density of this nanostructure in the anatase and rutile phases is 3.894, 4.250 and their gap is 3.3 eV and 3.1, respectively.

4.2. *Thermodynamic Properties of TiO2 Nanomaterials*

Rutile has a stable phase at high temperatures, but anatase and brookite (nanostructure) are common in natural and synthesized samples. By continuous heating and roughening, the deformation from anatase to brookite to rutile, brookite to anatase to rutile, anatase to rutile, and brookite to rutile is observed. This series of changes further implies equilibrium energies as a function of particle size. The enthalpy level of these three structures is different. In thermodynamics, stability can be obtained by coagulating anatase or boracite in small particle size. The crystal structure of titanium dioxide nanoparticles is highly dependent on how they are prepared. For smaller nanoparticles (smaller than 50 nm), more stable anatase is observed, which transforms into rutile at temperatures above 973 k. It has even been observed that this deformation occurs when the particle size reaches a certain value. For example, for particles larger than 14 nm, rutile is more stable than anatase. Phase stability in the thermodynamic state is discussed by Gibbs free energy ($\Delta G=\Delta H-T\Delta S$) relative to enthalpy. Rutile and anatase have the same enthalpy. Lee showed that the phase change of anatase to rutile occurred in the temperature range of 1073-973 k. Rutile and anatase particle sizes also increased with increasing temperature, but the growth rate was different. Rutile has a higher growth rate than anatase.

The X-ray diffraction property of TiO_2 XRD nanomaterials is effective in determining the crystal structure and crystallization as well as estimating the crystal size. According to the Sherer relation we have:

$$D = \frac{\lambda k}{\beta cos\theta} \qquad (1)$$

Where k is a dimensionless constant, two diffraction angles, λ X-ray wavelength and B total width at half the maximum peak diffraction (FWHM).

The crystalline size is determined by measuring the propagation of a particular peak in a diffraction pattern with a surface reflection from within the single crystal cell, which is inversely related to FWHM - the thinner the peak, the larger the fine crystal. The unique periodicity of the crystallite fields enhances the X-ray diffraction and leads to a longer and narrower peak. If the crystals are placed randomly or have a low periodicity, it is limited to a larger peak. Therefore, it is obvious that FWHM is related to the size of nanomaterials. XRD results for 2TiO nanoparticles and nanorods showed that the diffraction peaks become narrower as the nanoparticle size increases.

5. *Discussion*

5.1. *Use of Nanostructures to Improve the Efficiency of Polymer Solar Cells*

Recent research has shown that the performance of these devices depends on the type of nanostructure used in the active layer due to more efficient charge separation and transport of carriers in semiconductor materials. When the size or dimensions of a material are constantly changing from large to very small, the properties do not change in the first place. Then small changes begin until, when the size reaches below 100 nm, dramatic changes in properties occur. If in these materials the dimensions are reduced to the nanoscale in only one dimension while the other two dimensions remain large, we reach a structure known as the quantum well. If two dimensions are reduced to the nanoscale, and the different dimension remains large, the resulting structure is a quantum wire. At the end of the size reduction process, when all three dimensions reach the scale below the nanometer, a quantum dot is obtained; in other words, the quantum dots can be called zero-dimensional nanostructures. Hybrid photovoltaic cells based on a combination of nanocrystals and polymers have significant potential for cost reduction and growing solar power conversion. Because the ratio of surface area to particle volume increases with decreasing particles, the use of nanostructures in the active layer of the solar cell as a receiver or donor or in electrodes as a carrier collector is very useful. Nanotechnology, in addition to increasing energy conversion efficiency, is also considered in terms of reducing manufacturing costs.

Pigmented Titanium-Based Pigmented Solar Cell

Among organic solar cells, pigment hybrid solar cells are highly efficient. Pigment cells the photoelectrochemical solar cell is based on the light sensitization of titania nanocrystals by pigment. A key feature of this type of solar cell is the use of titanium nanocrystals due to its large surface-to-volume ratio. In this type of solar cell, cell performance can be improved by replacing inorganic nanoparticles or quantum dots instead of pigments. Inorganic nanoparticles instead of organic pigments, can indicate a suitable gap and thus the expansion of absorption. Nanocrystals have a high absorption coefficient due to their inherent dipole moment, which leads to rapid charge separation and relative stability of inorganic materials. Besides, due to the effects of quantum band constraint, quantum dot semiconductors can be controlled by controlling the particle size, and the optical properties can be changed for further overlap with the absorption range of the solar spectrum.

Organic Solar Cell Inverted Structure Based on Titanium

As we know, the larger the thickness of the polymer film, the higher the adsorption rate, but due to the small length of the exciton distribution, effective separation and transport of carriers is prevented. One practical way to overcome this problem is to increase the donor-acceptor interface by introducing

nanostructures that help collect and transport carriers. A useful method is to fill the pores of titania nanotube arrays with the organic semiconductor material. For this purpose, a polymer solar cell with an inverted structure was made with titania nanotubes as an electron transfer layer (Figure 2). A combination of poly (3-hexathiophene) and (, 66) -phenyl-61 C butyric acid methyl ester was considered as the active layer. The results show that these nanotubes provide vertical charge transfer from the active layer to the electrode. The measured parameters for this type of solar cell include a short-circuit current density of 10.96 $^{2-}$mAcm, an open-circuit voltage of 0.59, an efficiency factor of 0.42, and an energy conversion efficiency of 2.71%.

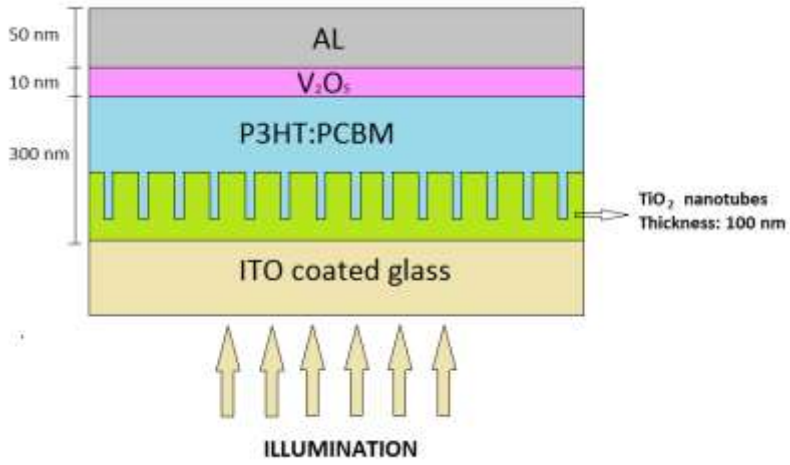

Fig 2. Reverse polymer solar cell structure with titania nanotype

In organic solar cell inverted structure based on titanium thin film, the electrical parameters were short-circuited current density of 0.38 $^{2-}$mAcm, open circuit voltage 0.39 mV, efficiency factor 0.17 and efficiency 0.025%, respectively. When nanoprocessor film was used instead of thin film, the parameters were 2.42 $^{2-}$ mAcm , 0.50 mV, 30 and 0.36% efficiency, respectively.

Hybrid Solar Cell with Single Crystal Silicon Nanowires

Because organic matter alone does not transmit carriers well, instrument performance is limited by the low probability of exciton separation. For efficient mutation of carriers, nanostructured semiconductors are proposed in combination with organic materials, not only because they provide a more effective surface between organic and inorganic materials, but also because electrons transfer more rapidly in these semiconductors. For this purpose, many inorganic nanowires such as cadmium telluride, cadmium selenide, zinc oxide and titania were investigated. Cadmium telluride and cadmium selenide are harmful to the environment, and zinc oxide and titanium also have a gaffe band greater than 3 eV and cannot absorb the sun's spectrum well. To overcome this problem, silicon nanowires with a high absorption coefficient, which are good absorbers in the infrared spectrum and are compatible with the environment, were tested. Fullerene hybrid solar cell: poly (3-hexathiophene) and silicon nanowires are shown in Figure (3).

The measured characteristics for devices without silicon nanowires were short-circuited current density of 7.17^{2-}mAcm, open-circuit voltage of 414 mV, the efficiency factor of 0.407 and efficiency of 1.21%. The results showed that with the introduction of silicon nanowires, all parameters were improved

so that the short-circuit current density was 11.61 $^{2-}$mAcm, the open-circuit voltage was 425 mV, the efficiency factor was 0.39, and the efficiency was 1.93%. The increase in current in this tool can be explained by the following reasons:

3. Nanowires provide a direct path for the collection and transport of carriers.
4. The high density of these nanowires increases the silicon/poly (3-hexathiophene) interface and improves the exciton resolution.
5. Silicon nanowires can compensate for the absorption spectrum of the polymer composition by absorbing light in the infrared region.

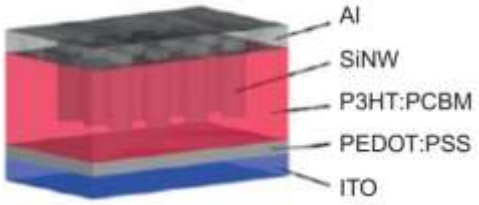

Fig. 3 Nanostructured silicon-based organic hybrid solar cell structure [1]

Hybrid Solar Cell with Cadmium Telluride Nanorods

Initially, Sarisif Tik reported the highest efficiency factor of 0.48 and an efficiency of 0.04% for fullerene hybrid solar cells and conjugated polymers. Further improvement of the hybrid solar cell was achieved by combining cadmium telluride/poly (3-hexathiophene) nanorods as the active layer. This instrument showed open-circuit voltage of 0.7 v, short circuit current of 5.7 mAcm, efficiency factor of 0.4 and efficiency of 1.7%. This cell has improved optical absorption compared to the previous cell due to these nanorods. A similar case with polymer-polymer (3-octyl thiophene) as an active ingredient in solar cells had an efficiency of 0.006%, and with the addition of cadmium telluride nanorods to this compound, the efficiency was improved to 0.06%. The structure of such a cell is shown in Figure (4).

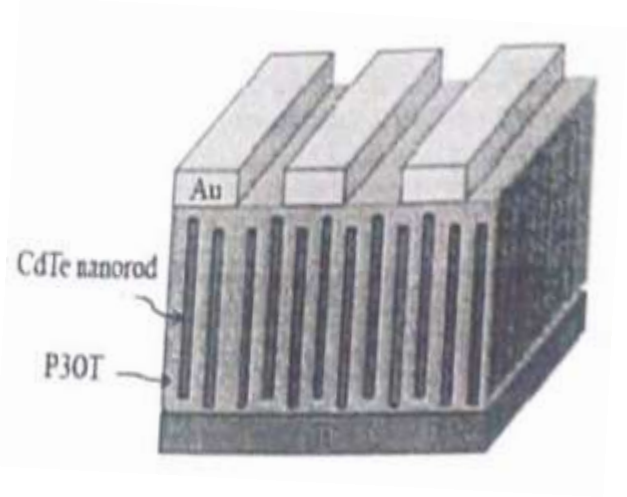

Fig. 4 Cd cadmium telluride/polymer poly (3-octyl thiophene) hybrid solar cell structure

The results show that the use of nanorods leads to better optical absorption, more efficient separation of excitons and transfer of electrons perpendicular to the film surface.

Polymer Solar Cell Based on Zinc Oxide and Titania Nanorods

The tool structure based on ZnO / P3HT: TiO_2 is shown in Figure (5-5). In this structure, zinc oxide nanorods are used as an electron transfer layer, and titanium/polymer nanorod hybrid is used as an active layer. A thicker layer of Russian zinc oxide arrays provides a path for the electrode surface to collect and transport carriers to the electrode. Titanium thinner nanorods that penetrate the polymer have a large interface with the polymer and lead to improved exciton separation and carrier transport.

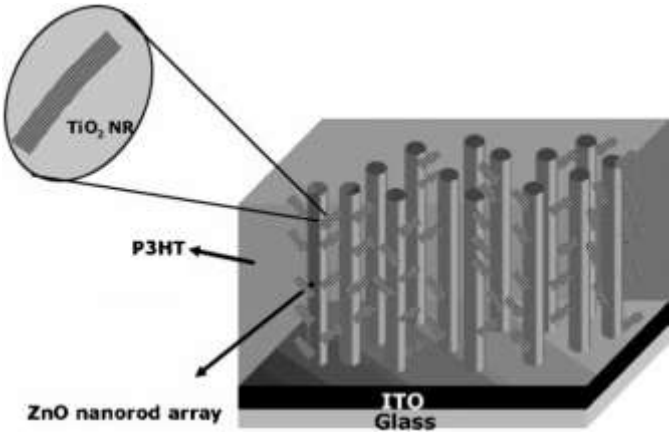

Fig. 5 Schematic of the structure of a hybrid solar cell based on ZnO/P3HT:TiO_2

Three instruments with different configurations were developed for comparison. The measured parameters of these tools are summarized in Table (1). Tool (I) ZnO / P3HT is based on a pure polymer film coated on zinc acid nanorods. Tool II with configuration (ZnO / P3HT: TiO_2) showed a 6-fold increase in the current density collected from the cell compared to the tool I due to the presence of titania nanorods. Tool III with configuration (ZnO / TiO_2 / P3HT: TiO_2) showing a thin film of titania nanorods on laminated zinc oxide nanorods showed an increase in current density compared to tool II This increase can be attributed to the addition of a titanium nanorod layer that prevents electrons from returning to the polymer and recombining with the pores.

Table 1. Parameters measured from various hybrid solar cell instruments based on zinc oxide nanorods

η(%)	FF(%)	$J_{sc}(mAcm^{-2})$	$V_{oc}(mV)$	Type of tool
0/04	40	0/30	335	I
0/29	39	1/96	380	II
0/31	35	2/20	400	III

From the photovoltaic performance of these devices with different configurations, it can be seen that the presence of titanium nanorods in the hybrid structure of zinc oxide / polymer improves the performance of the solar cell by increasing the effective surface area and transmission path.

References

[1] Kalita, G., Umeno, M., & Tanemura, M. (2014). Blend of Silicon Nanostructures and Conducting Polymers for Solar Cells. In Nanostructured Polymer Blends (pp. 495-508). William Andrew Publishing.

[2] Liu, J., Li, Y., Arumugam, S., Tudor, J., & Beeby, S. (2018). Investigation of low temperature processed titanium dioxide (TiO2) films for printed dye sensitized solar cells (DSSCs) for large area flexible applications. Materials Today: Proceedings, 5(5), 13846-13854.

[3] Sacco, A., Porro, S., Lamberti, A., Gerosa, M., Castellino, M., Chiodoni, A., & Bianco, S. (2014). Investigation of transport and recombination properties in graphene/titanium dioxide nanocomposite for dye-sensitized solar cell photoanodes. Electrochimica Acta, 131, 154-159.

[4] Fan, W., Tan, D., & Deng, W. (2011). Theoretical investigation of triphenylamine dye/titanium dioxide interface for dye-sensitized solar cells. Physical Chemistry Chemical Physics, 13(36), 16159-16167.

[5] Hosseinnezhad, M., Gharanjig, K., Yazdi, M. K., Zarrintaj, P., Moradian, S., Saeb, M. R., & Stadler, F. J. (2020). Dye-sensitized solar cells based on natural photosensitizers: A green view from Iran. Journal of Alloys and Compounds, 828, 154329.

[6] Yarmohamadi-Vasel, M., Modarresi-Alam, A. R., Noroozifar, M., & Hadavi, M. S. (2019). An investigation into the photovoltaic activity of a new nanocomposite of (polyaniline nanofibers)/(titanium dioxide nanoparticles) with different architectures. Synthetic Metals, 252, 50-61.

[7] Nikoobakht, A., Aghaei, J., Fallahzadeh-Abarghouei, H., & Hemmati, R. (2019). Flexible Co-Scheduling of Integrated Electrical and Gas Energy Networks under Continuous and Discrete Uncertainties. *Energy*.

[8] Badri-Koohi, B., Tavakkoli-Moghaddam, R., & Asghari, M. (2019). Optimizing Number and Locations of Alternative-Fuel Stations Using a Multi-Criteria Approach. Engineering, Technology & Applied Science Research, 9(1), 3715-3720.

[9] Badri-Koohi, B., & Tavakkoli-Moghaddam, R. (2012, July). Determining optimal number and locations of alternative-fuel stations with a multi-criteria approach. In 8th International Industrial Engineering Conference, Tehran, Iran.

[10] Khezri, M., & Rasmussen, K. J. R. (2019). An energy-based approach to buckling modal decomposition of thin-walled members with arbitrary cross sections, Part 1: Derivation. *Thin-Walled Structures*, *138*, 496-517.

[11] Khezri, M., & Rasmussen, K. J. R. (2019). An energy-based approach to buckling modal decomposition of thin-walled members with arbitrary cross-sections, Part 2: Modified global torsion modes, examples. *Thin-Walled Structures*, *138*, 518-531.

[12] Khezri, M., Bradford, M. A., & Vrcelj, Z. (2015). Application of RKP-FSM in the buckling and free vibration analysis of thin plates with abrupt thickness changes and internal supports. *International Journal for Numerical Methods in Engineering*, *104*(2), 125-156.

[13] Tehrani, M., Moshaei, M. H., & Sarvestani, A. S. (2017). Network polydispersity and deformation-induced damage in filled elastomers. Macromolecular Theory and Simulations, 26(6), 1700038.

[14] Moshaei, M. H., Tehrani, M., & Sarvestani, A. (2019). On stability of specific adhesion of particles to membranes in simple shear flow. Journal of biomechanical engineering, 141(1), 011005.

[15] Moshaei, M. H., Tehrani, M., & Sarvestani, A. (2019). Rolling adhesion of leukocytes on soft substrates: Does substrate stiffness matter?. *Journal of biomechanics*, *91*, 32-42.

[16] Nasr, A. K., Kashan, M. K., Maleki, A., Jafari, N., & Hashemi, H. (2020). Assessment of Barriers to Renewable Energy Development Using Stakeholders Approach. Entrepreneurship and Sustainability Issues, 7(3), 2526-2541.

[17] Kondori, M. Esmaeilirad, A. Baskin, B. Song, J. Wei, W. Chen, et al. Identifying catalytic active sites of trimolybdenum phosphide (Mo3P) for electrochemical hydrogen evolution. Advanced Energy Materials. 9 (2019) 1900516.

[18] Behjat, A., Jafari Nodoushan, F., Khoshroo, A., & Ghoshani, M. (2015). Study of the effect of Titanium dioxide nano particle size on efficiency of the dye-sensitized Solar cell using natural Pomegranate juice. Iranian Journal of Physics Research, 14(4), 361-367.
[19] Ashrafi, R., Azarbayjani, M., Cox, R., Futrell, B., Glass, J., Zarrabi, A., & Amirazar, A. (2019). Assessing the Performance of UFAD System in an Office Building Located In Various Climate Zones.
[20] Rastegarzadeh, S., Mahzoon, M., & Mohammadi, H. (2020). A novel modular designing for multi-ring flywheel rotor to optimize energy consumption in light metro trains. Energy, 206, 118092.
[21] Kazemi, A., & Yang, S. (2019). Atomistic Study of the Effect of Magnesium Dopants on the Strength of Nanocrystalline Aluminum. JOM, 71(4), 1209-1214.
[22] Kazemi, A. (2019). Atomistic Study of the Effect of Magnesium Dopants on Nancrystalline Aluminium (Doctoral dissertation).
[23] Asadi-Ojaee, S. S., Mirabi, A., Rad, A. S., Movaghgharnezhad, S., & Hallajian, S. (2019). Removal of Bismuth (III) ions from water solution using a cellulose-based nanocomposite: A detailed study by DFT and experimental insights. Journal of Molecular Liquids, 295, 111723.
[24] Chegeni, M., Pour, S. K., & Dizaji, B. F. (2019). Synthesis and characterization of novel antibacterial Sol-gel derived TiO2/Zn2TiO4/Ag nanocomposite as an active agent in Sunscreens. Ceramics International, 45(18), 24413–24418. doi: 10.1016/j.ceramint.2019.08.163.
[25] Kermani, H., & Rohrbach, A. (2018). Orientation-Control of Two Plasmonically Coupled Nanoparticles in an Optical Trap. ACS Photonics, 5(11), 4660-4667.
[26] Movaghgharnezhad, S., & Mirabi, A. (2019). Advanced Nanostructure Amplified Strategy for Voltammetric Determination of Folic Acid. Int. J. Electrochem. Sci, 14, 10956-10965.
[27] Moghadas, B., Solouk, A., & Sadeghi, D. (2020). Development of chitosan membrane using non-toxic crosslinkers for potential wound dressing applications. *Polymer Bulletin*, 1-11.
[28] Gupta, S., Singh, P., Moghadas, B., Grim, B. J., Kodibagkar, V. D., & Green, M. D. (2020). Synthesis of PEG and quaternary ammonium grafted silicone copolymers as nanoemulsifiers. *ACS Applied Polymer Materials*, *2*(5), 1856-1864.
[29] Kondori, A., Esmaeilirad, M., Baskin, A., Song, B., Wei, J., Chen, W., ... & Asadi, M. (2019). Identifying Catalytic Active Sites of Trimolybdenum Phosphide (Mo3P) for Electrochemical Hydrogen Evolution. Advanced Energy Materials, 9(22), 1900516.
[30] Chegeni, M., Pour, S. K., & Dizaji, B. F. (2019). Synthesis and characterization of novel antibacterial Sol-gel derived TiO2/Zn2TiO4/Ag nanocomposite as an active agent in Sunscreens. Ceramics International, 45(18), 24413–24418. doi: 10.1016/j.ceramint.2019.08.163.
[31] Ntiribinyange, M. S. (2016). *Degradation of textile wastewater using ultra-small B-Feooh/Tio2 heterojunction structure as a visible light photocatalyst* (Doctoral dissertation, Cape Peninsula University of Technology).
[32] Mohtor, N. H., Othman, M. H. D., Bakar, S. A., Kurniawan, T. A., Dzinun, H., Norddin, M. N. A. M., & Rajis, Z. (2018). Synthesis of nanostructured titanium dioxide layer onto kaolin hollow fibre membrane via hydrothermal method for decolourisation of reactive black 5. *Chemosphere*, *208*, 595-605.
[33] Asemani, H., Zareanshahraki, F., & Mannari, V. (2019). Design of hybrid nonisocyanate polyurethane coatings for advanced ambient temperature curing applications. Journal of Applied Polymer Science, 136(13), 47266.
[34] Peng, F., Cai, L., Huang, L., Yu, H., & Wang, H. (2008). Preparation of nitrogen-doped titanium dioxide with visible-light photocatalytic activity using a facile hydrothermal method. *journal of Physics and Chemistry of Solids*, *69*(7), 1657-1664.
[35] Kamei, M., & Mitsuhashi, T. (2000). Hydrophobic drawings on hydrophilic surfaces of single crystalline titanium dioxide: surface wettability control by mechanochemical treatment. *Surface Science*, *463*(1), L609-L612.

[36] Mohammadnejad, H., Liao, S., Marion, B. A., Pennell, K. D., & Abriola, L. M. (2020). Development and validation of a two-stage kinetic sorption model for polymer and surfactant transport in porous media. Environmental Science & Technology.
[37] Hassantabar, S., Wang, Z., & Jha, N. K. (2019). SCANN: Synthesis of compact and accurate neural networks. arXiv preprint arXiv:1904.09090.
[38] Hassantabar, S., Dai, X., & Jha, N. K. (2019). STEERAGE: Synthesis of Neural Networks Using Architecture Search and Grow-and-Prune Methods. arXiv preprint arXiv:1912.05831.
[39] Pianko-Oprych, P., Hosseini, S. M., & Jaworski, Z. (2016). Model development of integrated CPOx reformer and SOFC stack system. *Polish Journal of Chemical Technology*, *18*(4), 41-46.
[40] Bagheri, M., & Azmoodeh, M. (2019). Substrate Stiffness Changes Cell Rolling and Adhesion over L-selectin Coated Surface in a Viscous Shear Flow. arXiv preprint arXiv:1910.00002.

Copyrights